2018

Magnetic and magnetocaloric properties of Co2-xFexVGa Heusler alloys

K. Schroeder
South Dakota State University

J. Waybright
South Dakota State University

P. Kharel
University of Nebraska - Lincoln

W. Zhang
University of Nebraska - Lincoln

Shah R. Valloppilly
University of Nebraska-Lincoln, svalloppilly2@unl.edu

See next page for additional authors

Magnetic and magnetocaloric properties of $Co_{2-x}Fe_xVGa$ Heusler alloys

K. Schroeder,[1] J. Waybright,[1] P. Kharel,[1,2] W. Zhang,[2,3] S. Valloppilly,[2] J. Herran,[4] P. Lukashev,[5] Y. Huh,[1] R. Skomski,[2,3] and D. J. Sellmyer[2,3]
[1]*Department of Physics, South Dakota State University, Brookings, SD 57007, USA*
[2]*Nebraska Center for Materials and Nanoscience, University of Nebraska, Lincoln, NE 68588, USA*
[3]*Department of Physics and Astronomy, University of Nebraska, Lincoln, NE 68588, USA*
[4]*Department of Chemistry and Biochemistry, University of Northern Iowa, Cedar Falls, IA 50614, USA*
[5]*Department of Physics, University of Northern Iowa, Cedar Falls, IA 50614, USA*

(Presented 8 November 2017; received 26 September 2017; accepted 30 November 2017; published online 11 January 2018)

The magnetic and magnetocaloric properties of iron-substituted Co_2VGa alloys, $Co_{2-x}Fe_xVGa$ (x = 0, 0.1, 0.15, 0.2, 0.3), were investigated. The Fe-substituted samples, prepared by arc melting, melt spinning, and annealing, crystallized in the $L2_1$ Heusler structure, without any secondary phases. The Curie temperature and high-field magnetization at 50 K decreased from 345 K and 44 emu/g (1.90 μ_B/f.u.) for Co_2VGa to 275 K and 39 emu/g (1.66 μ_B/f.u.) for $Co_{1.7}Fe_{0.3}VGa$, respectively, but the maximum entropy change remained almost insensitive to Fe concentration for $x \leq 0.2$, the highest value being 3.3 J/kgK at 7 T for $Co_{1.85}Fe_{0.15}VGa$. First-principle calculations show that Co_2VGa retains its half-metallic band structure until at least 30% of the cobalt atoms are replaced by Fe atoms. The wide operating temperature window near room temperature and the lack of thermal and magnetic hysteresis are the interesting features of these materials for application in room-temperature magnetic refrigeration. https://doi.org/10.1063/1.5006646

I. INTRODUCTION

Heusler compounds and alloys have attracted recent attention because of their many interesting properties with prospects for spintronics, energy technology and magnetocaloric applications.[1–3] Additionally, the magnetic properties of these materials can be tuned to fit specific applications by adjusting the elemental composition. The majority of Heusler compounds are cubic but some of them also show tetragonal distortion with a potential for high perpendicular magnetic anisotropy.[4] For spintronic applications, Heusler compounds with half-metallic and spin-gapless semiconducting properties have been investigated. Especially, Co-based compounds including Co_2MnSi, Co_2FeSi and CoFeCrAl have shown promising properties such as high transport spin polarization at the Fermi level and Curie temperature much above room temperature.[5–7] One of the issues with the Heusler compounds is the difficulty of synthesizing them in completely ordered structures. Certain types of disorder are detrimental to half-metallic properties.[8,9] On the other hand, some Mn-based Heusler alloys, including Ni–Mn–In–(Co) shape-memory alloys, exhibit a giant magnetocaloric effect, parameterized by the magnetic entropy change ΔS_M and driven by structural transitions. However, the main obstacles to the application of these materials are the large hysteresis and limited operating temperature window.[10]

These considerations stimulated the current work, where we have investigated the magnetic and magnetocaloric properties of Co_2VGa-based alloys. Co_2VGa is predicted to be half-metallic in the ordered $L2_1$ structure.[11] Previous experimental results on polycrystalline bulk samples show that Co_2VGa can be synthesized in ordered $L2_1$ structure, which is ferromagnetic at room temperature with

Curie temperature of about 357 K.[12] Since its Curie temperature (T_C) is close to room temperature, we have tuned the T_C between 345 K and 275 K by replacing a fraction of Co with Fe, considering its potential for magnetocaloric applications. In this paper, we present our experimental investigation of the structural, magnetic and magnetocaloric properties of $Co_{2-x}Fe_xVGa$ (x = 0, 0.1, 0.15, 0.2, 0.3) compounds, perform first-principle calculations, and compare the experimentally observed data with the results of the calculations.

II. METHODS

A. Experimental methods

We investigated three sets of $Co_{2-x}Fe_xVGa$ samples: arc melted ingots, rapidly quenched ribbons and annealed ribbons. The ribbon samples were prepared by arc melting, rapid quenching in a melt spinner and annealing. First, $Co_{2-x}Fe_xVGa$ ingots were produced by arc melting high-purity elements in an argon atmosphere. The ribbon samples were then prepared by rapid quenching of induction-molten ingots onto the surface of a copper wheel rotating at a speed of 25 m/s. The ribbons were also annealed at 400 °C for 8 hours in a high-vacuum furnace. The crystal structures of the samples were investigated using powder x-ray diffraction (XRD) in Rigaku Miniflex and D Max B diffractometers with copper and cobalt Kα radiations. Magnetic properties were investigated using a Quantum Design VersaLab magnetometer and Physical Properties Measurement system (PPMS). The elemental compositions of the ribbons were determined using energy-dispersive X-ray spectroscopy (EDX) in FEI Nova NanoSEM450. The magnetic data from the arc melted ingots and rapidly quenched ribbons are very similar, so that we restrict ourselves to the results from rapidly quenched and annealed ribbons.

B. Computational methods

We performed density-functional calculations of bulk Heusler compound, $Co_{8-x}Fe_xV_4Ga_4$ (x = 0, 1, 2, 3, 4), using the projector augmented-wave method (PAW),[13] implemented in the Vienna *ab initio* simulation package (VASP)[14] within the generalized-gradient approximation (GGA).[15] The integration method[16] was used with a 0.05 eV width of smearing, along with a plane-wave cutoff energy of 500 eV and energy convergence criteria of 10^{-2} meV for atomic relaxation (resulting in the Hellmann–Feynman forces being less than 0.005 eV Å^{-1}) and 10^{-6} eV for the total energy and electronic-structure calculations. A k-point mesh of 12 × 12 × 12 points was used for the Brillouin-zone integration. The atomic relaxations were performed with a smaller k-mesh of 6 × 6 × 6 points. A 16-atom cell with periodic boundary conditions was used. For all ground-state calculations, the geometry was fully optimized to obtain equilibrium structures. Some of the results were obtained using the MedeA® software environment.[17]

III. RESULTS AND DISCUSSION

A. Experimental results

Figure 1(a) shows the cubic $L2_1$ crystal structure of Co_2VGa, and Fig. 1(b) show the room-temperature x-ray patterns of powder samples prepared by grinding the rapidly quenched ribbons. The samples are all single phase, and the presence of characteristic (111) and (200) peaks confirms that the Fe-substituted samples crystallize in the cubic $L2_1$ structure. The Co_2VGa parent alloy has negligible (111) and (200) peak intensities, indicating substantial A2 disorder. We compared experimental XRD powder patterns with powder XRD simulations of the respective compositions assuming ordered $L2_1$ structure, that is, Fe occupying a part of the Co sites. Additionally, as shown in table I the Fe substitution did not produce a noticeable change in the lattice parameter of Co_2VGa ($a \approx 5.786$ Å), probably due to very similar sizes of Fe and Co atoms. The annealing of the samples did not show any change in the crystal structure except a slight increase in the grain size.

Figure 2(a) shows the thermomagnetic curves of the as-quenched $Co_{2-x}Fe_xVGa$ ribbons between 50 K and 400 K. As shown in Fig. 2(a) and Table I, the T_C of Co_2VGa is 345 K, which is close to the previously reported value of 357 K.[12] This value of T_C decreases nearly linearly to 275 K as the

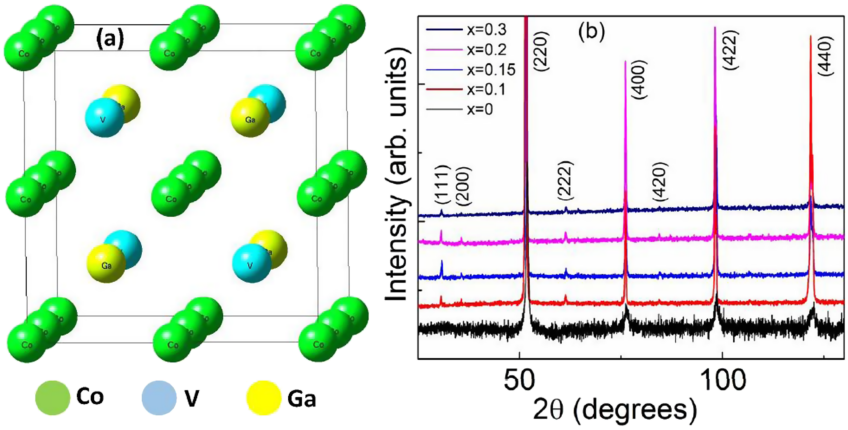

FIG. 1. (a) The cubic $L2_1$ crystal structure of Co_2VGa and (b) the powder XRD pattern of $Co_{2-x}Fe_xVGa$ (x = 0, 0.1, 0.15, 0.2 and 0.3) ribbons.

TABLE I. Magnetic properties of $Co_{2-x}Fe_xVGa$ as-quenched and annealed ribbons, and calculated magnetic moments per formula unit.

$Co_{2-x}Fe_x$		T_C (K)		Experimental M (emu/g) at 30 kOe	Calculated M (μ_B/f.u) $Co_{8-x}Fe_xV_4Ga_4$		ΔS_{max} (J/kg K) at 30 kOe	
VGa	a (Å)	As-quenched	Annealed	Annealed	x	M	As-quenched	Annealed
x = 0	5.7859	345	349	44 (1.90 μ_B/f.u.)	0	2.00	1.6	1.8
x = 0.1	5.7799	330	329	42 (1.80 μ_B/f.u.)	1	1.75	1.6	1.7
x = 0.15	5.7833	315	313	42 (1.80 μ_B/f.u.)	2	1.49	1.7	1.8
x = 0.2	5.7818	306	305	41 (1.75 μ_B/f.u.)	3	1.23	1.6	1.9
x = 0.3	5.7844	275	274	39 (1.66 μ_B/f.u.)	4	0.97	1.2	1.3

Fe concentration x increases to 0.3 (see inset of Fig. 2(a)). The magnetic transitions at T_c are sharper for the as quenched ribbons than for the bulk samples. The high-field magnetization (M_{3T}) measured at 50 K for both the as-quenched and annealed ribbons decrease with increasing x, from 44 emu/g (1.90 μ_B/f.u.) for Co_2VGa to 39 emu/g (1.66 μ_B/f.u.) for $Co_{1.7}Fe_{0.3}VGa$ (see Table I). The coercivities of the $Co_{2-x}Fe_xVGa$ alloys measured from the respective thermomagnetic curves recorded at 50 K are between 100 Oe and 200 Oe indicating that the samples are soft-magnetic. Furthermore, there was no thermal hysteresis in the $M(T)$ curves of all samples at T_C when the measurement was done in a complete cycle of heating and cooling between 50 K and 400 K, indicating a second-order magnetic

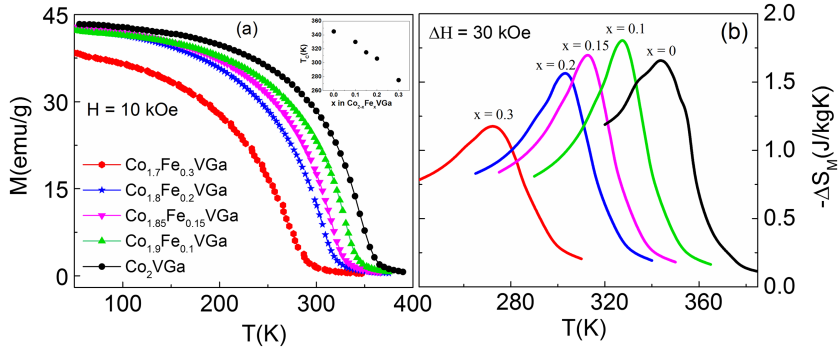

FIG. 2. (a) Thermomagnetic curves and (b) entropy change ΔS_M as a function of temperature for $Co_{2-x}Fe_xVGa$ (x = 0, 0.1, 0.15, 0.2 and 0.3) ribbons. The inset of Fig. 2(a) shows the T_c as a function of x.

transition. As shown in the table I, annealing of the samples did not produce significant change in the magnetic properties of the ribbon samples.

Since the Curie temperatures of the $Co_{2-x}Fe_xVGa$ alloys range from 275 K to 345 K, it is interesting to find if these materials possess potential for magnetocaloric applications. We determined entropy changes in these materials from respective isothermal magnetization curves recorded at several temperatures near Tc using the Maxwell's thermodynamic relation $S_M(T,H) = \int_0^H \left(\frac{\partial M}{\partial T}\right)_H dH$. Figure 2(b) shows the magnetic entropy change ΔS_M calculated for $\Delta H = 30$ kOe at temperatures near the respective T_C of the rapidly quenched $Co_{2-x}Fe_xVGa$ ribbons. The maximum values of magnetic entropy change $\Delta S_{M,max}$ for both the rapidly quenched and annealed ribbons are listed in Table I as well. As shown in the table, all samples show relatively small values of $\Delta S_{M,max}$ between 1.3 and 1.9 J/kgK. Although there is a significant change in the T_C due to Fe substitution, the $\Delta S_{M,max}$ remains almost insensitive to the Fe concentration between $x = 0$ and $x = 0.2$. We also measured ΔS_M at higher fields up to 70 kOe and found that $\Delta S_{M,max}$ increases with increasing ΔH reaching 3.3 J/kg K for $Co_{1.85}Fe_{0.15}VGa$ at $\Delta H = 70$ kOe. The heat treatment slightly increased the values of $\Delta S_{M,max}$ of these samples.

B. Computational results

In order to analyze the electronic, structural, and magnetic properties of $Co_{2-x}Fe_xVGa$, we performed first-principle calculations using a 16-atom $Co_{8-x}Fe_xV_4Ga_4$ supercell in the ordered $L2_1$ structure, see Fig. 1(a). The Fe concentration was varied between $x = 0$ and $x = 4$ in the supercell, which corresponds to varying x between 0 and 0.5 per formula unit. We considered few representative configurations of Fe substitution, excluding the possibility of Fe "cluttering", i.e. we did not consider cells with all Fe atoms being nearest neighbors. With this approach, results reported below are rather robust, i.e. nearly independent from the choice of the particular configuration.

Figure 3(a) shows calculated element- and spin-resolved densities of states (DOS) for $Co_8V_4Ga_4$ for the optimized atomic positions. The calculated lattice constant for this cell is 5.752 Å, and the electronic structure is half-metallic, with metallic spin-up and insulating spin-down behavior. The top of the spin-down valence band is almost exclusively filled with Co states, while the lowest unoccupied spin-down states and spin-up states near the Fermi level have comparable contributions from cobalt and vanadium. The contribution from Ga to the total DOS near Fermi level is negligible. The energy gap of the minority-spin states is about 0.5 eV.

The calculated lattice constant (a) of $Co_{8-x}Fe_xV_4Ga_4$ exhibits a very small uniform decrease as the Fe content is increased, but this change is almost negligible, consistent with our experimental results.

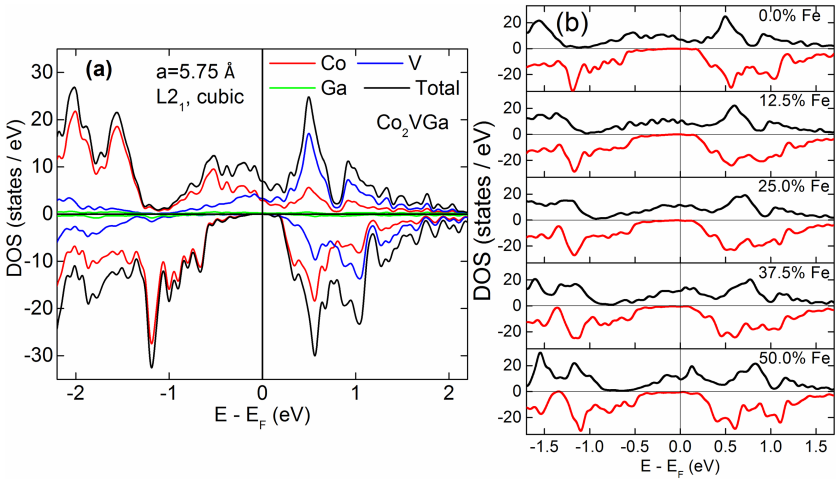

FIG. 3. (a) Atom- and spin-resolved densities of states (DOS) of fully ordered $L2_1$ $Co_8V_4Ga_4$. The atomic contributions are color-coded as indicated in the figure. (b) Calculated spin-resolved total DOS of $Co_{8-x}Fe_xV_4Ga_4$, as a function of x. Fe percentage is indicated in the figure. Positive DOS corresponds to spin-up, negative DOS to spin-down states.

In particular, as the Fe percentage increases from 0.0% to 50.0%, the lattice constant decreases from 5.752 Å to 5.735 Å. The total magnetic moment of $Co_{8-x}Fe_xV_4Ga_4$ decreases linearly with increasing Fe content, which is also consistent with the experimental results. All calculated total magnetic moments for small Fe concentrations have integer (or nearly integer) values per supercell, i.e. 8.0 μ_B for $Co_8V_4Ga_4$, 7.0 μ_B for $Co_7Fe_1V_4Ga_4$, 5.98 μ_B for $Co_6Fe_2V_4Ga_4$, 4.93 μ_B for $Co_5Fe_3V_4Ga_4$, and 3.88 μ_B for $Co_4Fe_4V_4Ga_4$, where all values are for a supercell. The main contributions to the total magnetic moment come from Co and Fe, but there is also a small induced magnetic moment on vanadium. The overall magnetic structure for all considered Fe concentrations is ferromagnetic. The reduction of the total magnetic moment with Fe substitution is caused by hybridization of Fe and Co orbitals, which induces the overall reduction of the local atomic magnetic moments in the vicinity of Fe, but does not result in an antiferromagnetic or ferrimagnetic transition.

The integer magnetic moment is a signature of half-metallicity. In particular, since the Fermi energy of $Co_{8-x}Fe_xV_4Ga_4$ is positioned in the spin-down band gap, all minority-spin states in the valence band are occupied, and thus their total number is an integer. This also causes the total magnetic moment to be an integer because of the integer total valence charge.[18] Furthermore, as the concentration of Fe increases (higher than about 30%), the deviations from the integer total magnetic moment become significant. Thus, our calculations indicate that for Fe concentrations of up to 30%, ordered $Co_{8-x}Fe_xV_4Ga_4$ is half-metallic, but for higher Fe concentration the spin polarization at the Fermi level could be slightly smaller than 100%.

Figure 3(b) shows the calculated spin-resolved total DOS of $Co_{8-x}Fe_xV_4Ga_4$ as a function of x. As shown in the figure, increasing Fe content does not significantly modify the half-metallic properties of this material, consistent with calculated integer (or nearly integer) values of the total magnetic moment. Moreover, qualitatively both majority- and minority-spin DOS are almost insensitive to the replacement of Co with Fe. Additionally, based on our calculated magnetic moment values, we expect that for higher Fe concentration (more than 30%) the spin polarization at the Fermi level could be slightly smaller than 100%. These deviations from half-metallicity for higher Fe concentrations are too small to be visible on the DOS plot (see bottom two panels of Fig. 3(b)).

IV. CONCLUSIONS

The $L2_1$ ordered $Co_{2-x}Fe_xVGa$ Heusler alloys were synthesized using arc melting, melt spinning and annealing. The partial substitution of Fe for Co in Co_2VGa produced significant change in the saturation magnetization and Curie temperature. The Curie temperature and high-field magnetization at 50 K decreased from 345 K and 44 emu/g (1.90 μ_B/f.u.) for Co_2VGa to 275 K and 39 emu/g (1.66 μ_B/f.u.) for $Co_{1.7}Fe_{0.3}VGa$, respectively, but the maximum entropy change remained almost insensitive to Fe concentration for $x \leq 0.2$. The first-principle calculations show that Co_2VGa retains its half-metallic band structure until at least 30% of the cobalt atoms are replaced with Fe atoms. Although the measured value of $\Delta S_{M,max}$ is small, the wide operating temperature window near room temperature, lack of both thermal and magnetic hysteresis and robustness against heat treatment indicate that $Co_{2-x}Fe_xVGa$ compounds are interesting to further investigate for magnetocaloric applications. Additionally, the robust half-metallic band structure with large band gap of about 0.5 eV show their potential for spintronic applications as well.

ACKNOWLEDGMENTS

This work at Nebraska is partially supported by NSF-DMREF: SusChEM (Award Number: 1436385). The experimental research was performed in part in the Nebraska Nanoscale Facility: National Nanotechnology Coordinated Infrastructure and the Nebraska Center for Materials and Nanoscience, which are supported by the NSF under Award ECCS: 1542182, and the Nebraska Research Initiative. The work at South Dakota State University is supported by Research/Scholarship Support Fund, Office of Research Assurance & Sponsored Programs. The work at University of Northern Iowa is supported by Pre-Tenure Grant from the Office of the Provost and Executive Vice President for Academic Affairs, as well as from the UNI Faculty Summer Fellowship.

[1] T. Graf, C. Felser, and S. S. P. Parkin, Prog. Solid State Chem. **39**, 1 (2011).
[2] S. Ouardi, G. H. Fecher, and C. Felser, Phys. Rev. Lett. **110**, 100401 (2013).
[3] J. Liu, T. Gottschall, K. P. Skokov, J. D. Moore, and O. Gutfleisch, Nat. Mater. **11**, 620 (2012).
[4] J. Winterlik, S. Chadov, A. Gupta, V. Alijani, T. Gasi, K. Filsinger, B. Balke, G. H. Fecher, C. A. Jenkins, F. Casper, J. Kübler, G. Liu, L. Gao, S. S. P. Parkin, and C. Felser, Adv. Mater. **24**, 6283 (2012).
[5] S. Oki, K. Masaki, N. Hashimoto, S. Yamada, M. Miyata, M. Miyao, T. Kimura, and K. Hamaya, Phys. Rev. B **86**, 174412 (2012).
[6] M. Jourdan, J. Minár, J. Braun, A. Kronenberg, S. Chadov, B. Balke, A. Gloskovskii, M. Kolbe, H. J. Elmers, G. Schönhense, H. Ebert, C. Felser, and M. Kläui, Nat. Commun. **5**, 3974 (2014).
[7] Y. Jin, P. Kharel, S. R. Valloppilly, X.-Z. Li, D. R. Kim, G. J. Zhao, T. Y. Chen, R. Choudhary, A. Kashyap, R. Skomski, and D. J. Sellmyer, Appl. Phys. Lett. **109**, 142410 (2016).
[8] Z. Gercsi and K. Hono, J. Phys. Condens. Matter **19**, 326216 (2007).
[9] Y. Jin, R. Skomski, P. Kharel, S. R. Valloppilly, and D. J. Sellmyer, AIP Adv. **7**, 055834 (2017).
[10] J. Liu, T. Gottschall, K. P. Skokov, J. D. Moore, and O. Gutfleisch, Nat. Mater. **11**, 620 (2012).
[11] Y. Miura, M. Shirai, and K. Nagao, J. Appl. Phys. **99**, 08J112 (2006).
[12] T. Kanomata, Y. Chieda, K. Endo, H. Okada, M. Nagasako, K. Kobayashi, R. Kainuma, R. Y. Umetsu, H. Takahashi, Y. Furutani, H. Nishihara, K. Abe, Y. Miura, and M. Shirai, Phys. Rev. B **82**, 144415 (2010).
[13] P. E. Blöchl, Phys. Rev. B **50**(24), 17953 (1994).
[14] G. Kresse and D. Joubert, Phys. Rev. B **59**(3), 1758 (1999).
[15] J. P. Perdew, K. Burke, and M. Ernzerhof, Physical Review Letters **77**(18), 3865 (1996).
[16] M. Methfessel and A. T. Paxton, Physical Review B **40**(6), 3616 (1989).
[17] MedeA® Version 2.19. MedeA® is a registered trademark of Materials Design, Inc. Angel Fire, New Mexico, USA.
[18] I. Tutic, J. Herran, B. Staten, P. Gray, T. Paudel, A. Sokolov, E. Tsymbal, and P. Lukashev, J. Phys. Condens. Matter **29**, 075801 (2017).